DIAGENESIS AND DISSOLUTION AT SINTER ISLAND (456 YRS BP), TAUPO VOLCANIC ZONE: SILICA STARS AND THE BIRTH OF QUARTZ

K.A.CAMPBELL[1] B.Y. LYNNE[1]
Scientist, Geology Programme, University of Auckland, NZ.

Total No of pages (Excluding Cover Page) = 7

[1]University of Auckland, Geology Programme, Chemistry Building, 23 Symonds Street, Auckland, N.Z.
Ph. +64-9-373-7599

DIAGENESIS AND DISSOLUTION AT SINTER ISLAND (456 YRS BP), TAUPO VOLCANIC ZONE: SILICA STARS AND THE BIRTH OF QUARTZ

K.A. CAMPBELL[1], B.Y. LYNNE[1]
[1] Geology Programme, University of Auckland, Auckland, New Zealand

SUMMARY – Sinter Island on Lake Ohakuri (10 m x 7 m, ~3 m above lake level) in the Orakei Korako geothermal area, Taupo Volcanic Zone, New Zealand, contains a large extinct vent, domal stromatolites and bedded sinter rich in microbial filaments. Despite its young age (456 ± 35 years BP), this ancient hot-spring deposit preserves the complete diagenetic sequence of silica phase mineralogies, confirmed by X-ray diffractometry, from opal-A to opal-CT to opal-C + quartz. Corresponding nano- to micron-scale morphologies include spheres and vitreous silica botryoids, bladed lepispheres, and merged irregular silica rods. Incipient 'fuzzy' quartz is represented by rows of criss-crossing rods/blades that are aligned along the c-axis, but showing the typical external habit of microcrystalline quartz. No microbial fabrics are evident in quartzose samples. The deposit also experienced spatially patchy dissolution, resulting in formation of unusual morphological features for some opal-A portions of the sinter. Three intervals of silicification (thin encrusting, thick botryoidal, cemented granular cavity-fill) occurred around filament clusters during alkali-chloride thermal discharge to create a moderately dense opaline deposit. Subsequent acidic conditions (acidic steam condensate or ascending acidic spring) ensued within the deposit, whereby dissolution preferentially removed the last-formed silica to expose the underlying filaments in cavities. Continuing corrosion freed silica spheres from the encrusted filaments to accumulate loosely in the vugs. Where touching, the spheres then merged via linking, double-annular necks among adjacent spheres. Further dissolution reduced sphere sizes concavely inward and extended lengths of the connecting neck-points to develop star-shaped patterns with "t-joints." The multi-pointed stars eventually broke loose as necks thinned and sharpened during further corrosion, and many likely dissolved completely. Solubility at the negative radius of curvature of the neck between spheres is less than elsewhere on the spheres (Iler, 1979). Therefore, the lower the solubility, the easier it would have been for the neck area to dissolve, and necks also would have been the first areas to be attacked by dissolution. The change to acidic conditions likely accelerated diagenesis of the siliceous mass, to produce quartz in less than 500 years.

1. INTRODUCTION

The Orakei Korako geothermal field is situated approximately 25 km north of Taupo in the Taupo Volcanic Zone, New Zealand. The field straddles the Waikato River, now submerged by Lake Ohakuri, with most surface activity located on its eastern side and controlled by faults (Fig. 1; Lloyd, 1972; Bignall, 1991; Simmons and Browne, 1991). Hot springs – both alkali chloride and acid – as well as geysers, fumaroles, steaming and rotting ground, hydrothermal explosion breccias, coloured clays and mud pools occur in the bush-clad terrain and along the lake margin near the Orakei Korako resort (Lloyd, 1972; Hamlin, 1999). Expansive sinter terraces developed locally in the past, when discharging alkali chloride springs deposited silica at the extinct Umukuri site (5×10^5 m^3 sinter volume; 4694 to 1571 ± 40 years BP; Campbell et al., 2001; Campbell unpublished data), 1 km SW of the resort. Old sinter deposits also underpin the Rainbow/Emerald, Golden Fleece, Artist's Palette and Kurapai/Ellan Vannin sinter terraces in the resort area (Fig. 1; 6276 ± 35 years BP; Lloyd, 1972; Hamlin, 1999; Campbell, unpublished data). Smaller outflows emerge today from alkali chloride springs at several Orakei Korako sites, and at Sinter Waterfall 1.5 km to the south (Hamlin, 1999; Currie, 2005). However, most present surface geothermal activity is derived from acid conditions caused by infiltration of steam acid condensate or ascending acid springs (cf. Lloyd, 1972; Hamlin, 1999; Lynne et al., 2006a).

Sinter Island (Hamlin, 1999) is located on Lake Ohakuri about 600 m upstream and south of the main tourist area and 40 m from the eastern bank of the lake (Fig. 1). The Island comprises an extinct siliceous hot-spring deposit from earlier alkali chloride spring activity (456 ± 35 years BP). It is triangular in shape, 7 m × 10 m in areal extent, and contains a large indentation at a fossil vent on its eastern side. The sinter is emergent up to ~ 3 m above the lake surface at high water mark, with daily, dam-controlled fluctuations of water levels to ±~0.5 m. The extent of the sinter beneath the lake surface is unknown. The exposed sinter is relatively flat bedded, and contains scattered domal stromatolites on its western margin, and vent geyserite on its eastern side. Several submerged, active springs also are situated on the lake bottom around the study site,

causing convection plumes and bubble trains that break the lake surface around Sinter Island.

As shown herein, the sinter deposit has undergone steam acid overprinting, which has accelerated silica diagenesis and affected preservation of the earlier-formed microbial fabrics. Dissolution has also modified the opaline portions of the deposit, to develop unusual 'silica stars' which are similar in morphology to pollen grains, but created by inorganic processes. Although silica originally templated upon and entombed microbial filaments, build up of a dense opaline deposit obscured their textural biosignals; whereas dissolution obliterated them completely.

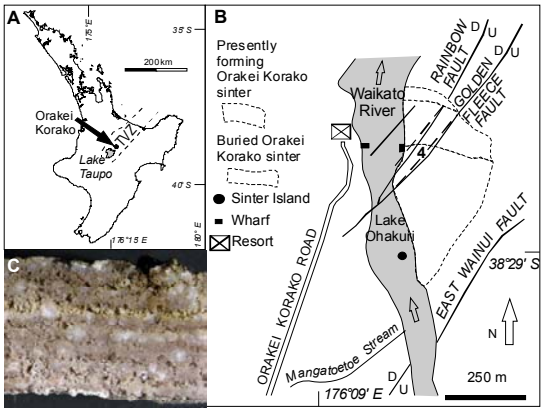

Figure 1: A) Taupo Volcanic Zone in the central North Island. B) Location of Sinter Island in the Orakei Korako geothermal field. Also shown are major faults, and presently forming and old sinter sites. C) Sinter hand sample of opal-A mineralogy from Sinter Island.

2. METHODS

Sinter Island and other extinct sinter deposits around Orakei Korako were dated by calibrated ^{14}C analysis of entombed organic matter, utilizing accelerator mass spectrometry at the Rafter Radiocarbon Laboratory, GNS Science Ltd., Lower Hutt, New Zealand. Extraction methods are described in Lynne et al. (2003). X-ray powder diffraction analysis (XRPD) was used to determine silica phase mineralogy. Techniques are described in Lynne et al. (2005). The shape of the XRPD trace and its full width at half maximum (FWHM) indicate silica phases present from opal-A to quartz. FWHM decreases with increasing mineralogical maturity (e.g., Lynne et al., 2006b). Scanning electron microscopy (SEM) allowed detailed, submicron-scale mapping of morphological changes in the siliceous sinter matrix during diagenesis and/or dissolution. Sample preparation and operating conditions of the scanning electron microscope are outlined in Lynne et al. (2005).

3. RESULTS

3.1 Accelerated diagenesis leading to 'birth of quartz'

The Sinter Island deposit is young (456 ± 35 yrs BP), and yet preserves the entire gamut of silica mineral phase transformations known to occur during diagenesis, from opal-A to opal-CT to opal-C to quartz (Table 1; Figure 2; cf. Lynne et al., 2005), a mineralogical transition once thought to take thousands of years to eventuate (Herdianita et al., 2000). Rates of sinter diagenesis are affected by the presence of accessory components (e.g., organic matter, carbonate, iron), and by post-depositional environment, such as overprinting by acidic conditions (cf. Herdianita et al., 2000; Lynne et al., 2006b). At Sinter Island, fresh siliceous deposits consist of noncrystalline opal-A microspheres (Fig. 2A). During early diagenesis, the microspheres merged into opaline botryoids, and were modified by solution-reprecipitation and structural water loss to form paracrystalline bladed lepispheres of opal-CT (Fig. 2B, 2C), then irregular nanostructures of opal-C (Fig. 2D), and finally microcrystals of quartz (Lynne et al., 2006b). The Sinter Island deposit not only captures this classic mineralogical-morphological continuum, but it also provides new observations on the manner in which 'juvenile quartz' emerges from the sinter matrix during diagenesis. In particular, opal-C nanostructures reorganize themselves toward future c-axes of quartz (e.g. fig. 2C4 in Lynne et al., 2006b). Incipient 'fuzzy quartz' grows inward from vugs, showing internal, strongly aligned criss-cross patterns (Fig. 2E) and external macro-morphologic habits of typical quartz microcrystals (e.g., Fig. 2F). Lynne et al. (in review) further explore the crystallographic underpinnings of increasing mineralogical maturity in sinter deposits, including Sinter Island.

3.2 Three stages of silicification at Sinter Island

At Sinter Island, silicification during alkali chloride discharge (at least 450 years BP) developed in three stages, which are well-preserved in the mineralogically immature, opal-A portions of the deposit (Figs. 1C, 3). Silica first templated upon filamentous microbial mats in thin coatings (~1-5 μm thick; Figs. 2A, 3A). The coatings comprise merging opaline silica microspheres that evenly encrusted the filaments (Fig. 3A). This first silicification event probably occurred quite early in diagenesis, as many filamentous microfossils appear to be preserved in life position, in aligned aggregations or networks. Second, thick botryoidal opaline cement (to 10 μm) agglomerated around clusters of silicified filament molds (Fig. 3B). The third silicification event filled remaining pore spaces around the silicified filaments with granular silica (Fig. 3C; to 300 nm diameter) that became further cemented

to create a moderately dense deposit (Fig. 3D-F). The original microbial surfaces upon which mineralization proceeded can be recognized texturally throughout the three phases of silicification (Fig. 3D-F). However, in places, only faint ghosts of the filaments are apparent in some of the more densely infilled areas of the deposit (e.g., Fig. 3D, 3F).

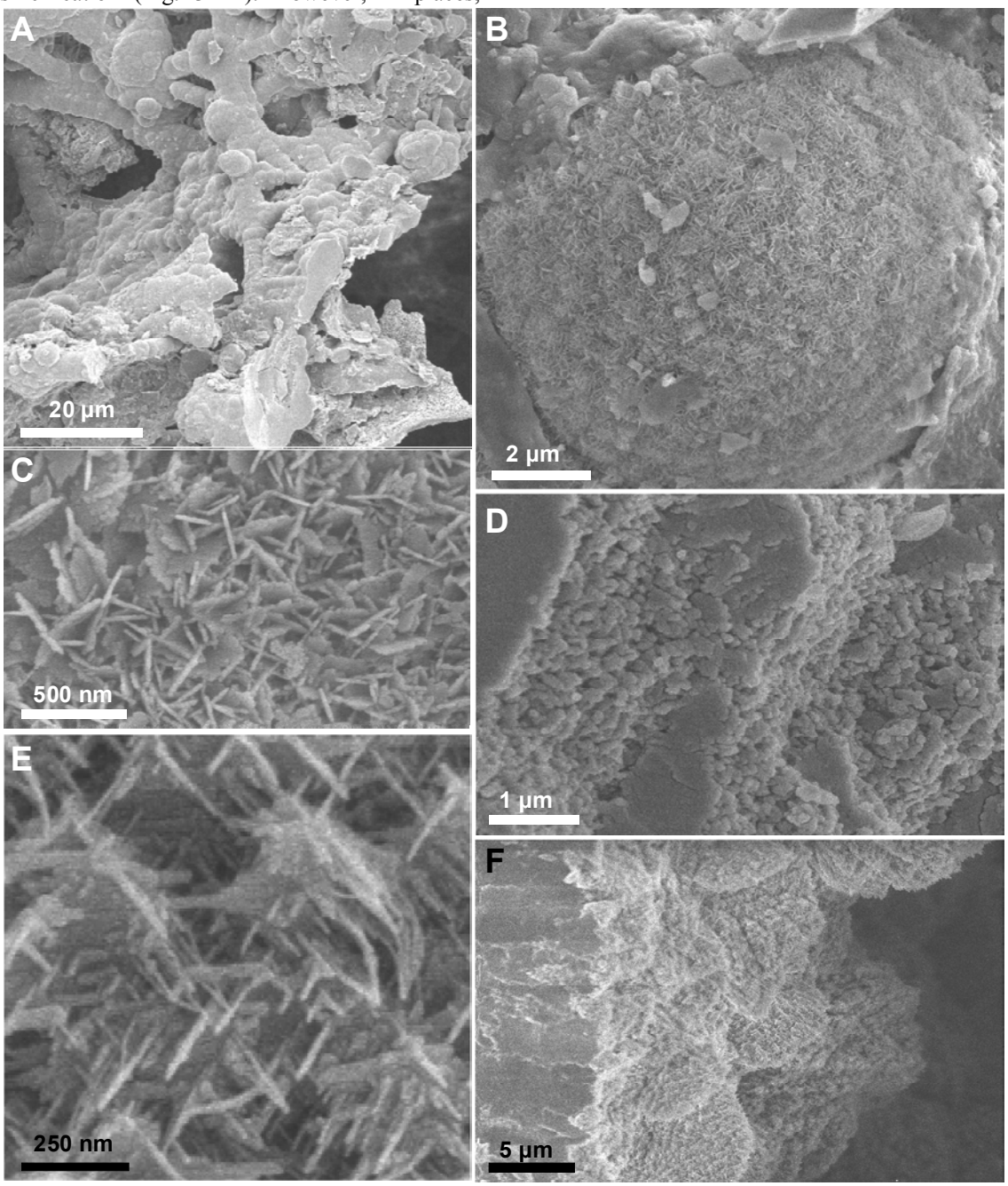

Figure 2: Sinter diagenesis morphologies at Sinter Island, from opal-A microspheres to fuzzy incipient quartz. A) Smooth silica spheres and thin coatings upon microbial filaments; B) opal-CT bladed lepisphere; C) detail of jagged cross-hatched blades of a lepisphere of opal-CT mineralogy; D) stepped horizons in matrix of merging opal-C nanostructures; E) sharp criss-cross pattern of incipient quartz showing alignment of nanostructures; F) criss-cross structures of (E) emerging within larger incipient quartz microcrystals growing into a vug.

Table 1: Range of full width at half maximum (FWHM) values from XRPD data set for Sinter Island samples, from opal to quartz

Silica phase	Number of samples	FWHM (º2Θ)
Opal-A	19	7.50-6.05
Opal-A/CT	10	6.00-5.80
Opal-CT	5	2.50-0.80
Opal-C	7	0.95-0.70

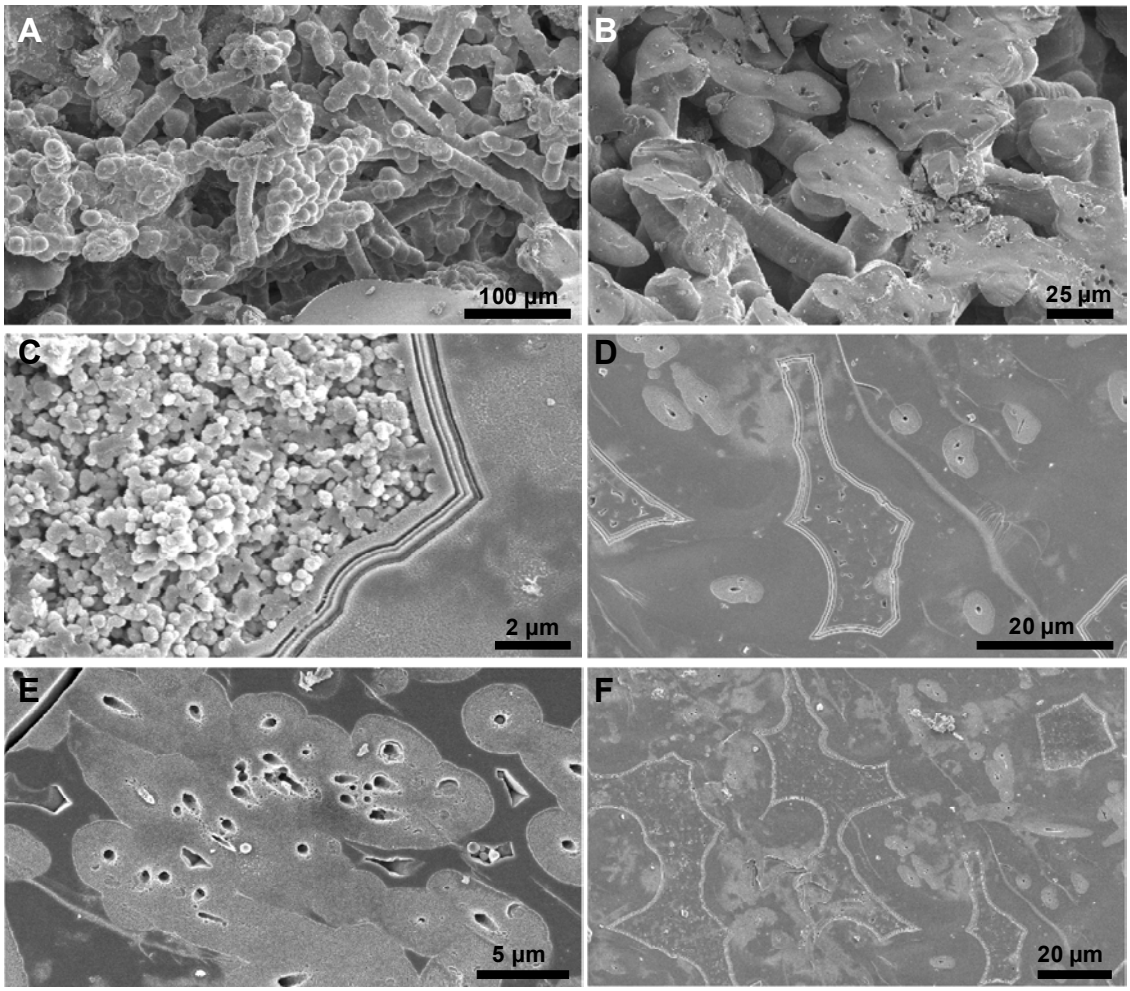

Figure 3: Three-stage sequence of silicification of microbial mats from alkali chloride-spring discharge at Sinter Island. A) Microbial filaments grew in thermal outflow and became encrusted with silica spheres and thin silica coatings (Stage I silicification). B) Thickly encrusted filaments created a botryoidal sinter fabric in Stage II silicification. C) Pore spaces around silicified filament clusters were subsequently infilled with granular silica in Stage III silicification. D-F) Further cementation of the microbial filaments and their encrusting silica into a solid sinter mass.

3.3 Post-depositional sinter dissolution and formation of 'silica stars'

Following the alkali chloride spring discharge phase and its three associated silicification events (section 3.2), acidic conditions ensued. The products of acid overprinting on the opaline portions of the sinter are evident from dissolution textures (surface pitting, thinning of silica encrustations), and emergence of earlier silica morphologies that had been covered by later silicification stages (e.g., Figs. 4A, 4B). Hence, old micro-cavities and silicified filaments reappeared, and the once-buried silica spheres became freed from the matrix (originally formed at the first stage of silicification), to drop into vugs and pits (Fig. 4A, 4B). Where adjacent spheres were in physical contact, their surfaces then merged into thin, slightly pinched necks (to ~5 µm wide; Fig. 4C-E). With further dissolution, small spheres disappeared more rapidly than large spheres, and the connecting necks thinned to "t-joints" and developed double annular rings (Fig. 4E). Star-shaped arrays of interconnected silica structures with multiple points subsequently arose as the mace-like balls shrank inward and the connecting 'necks' further thinned and elongated (Fig. 4F-H). These sharp-pointed silica stars eventually disconnected from adjoining structures to gather freely in piles within cavities (Fig. 4G). At this stage in the dissolution process, the silica stars appear quite similar to some types of pollen grains (e.g., Moar, 1993). In places where dissolution proceeded even further, the silica stars themselves shrank in size and exhibited blunted tips. Presumably some disappeared completely where localized acid conditions persisted long enough. Such unusual morphological features may have gone unrecognized or have been

misidentified as pollen grains in other sinter deposits.

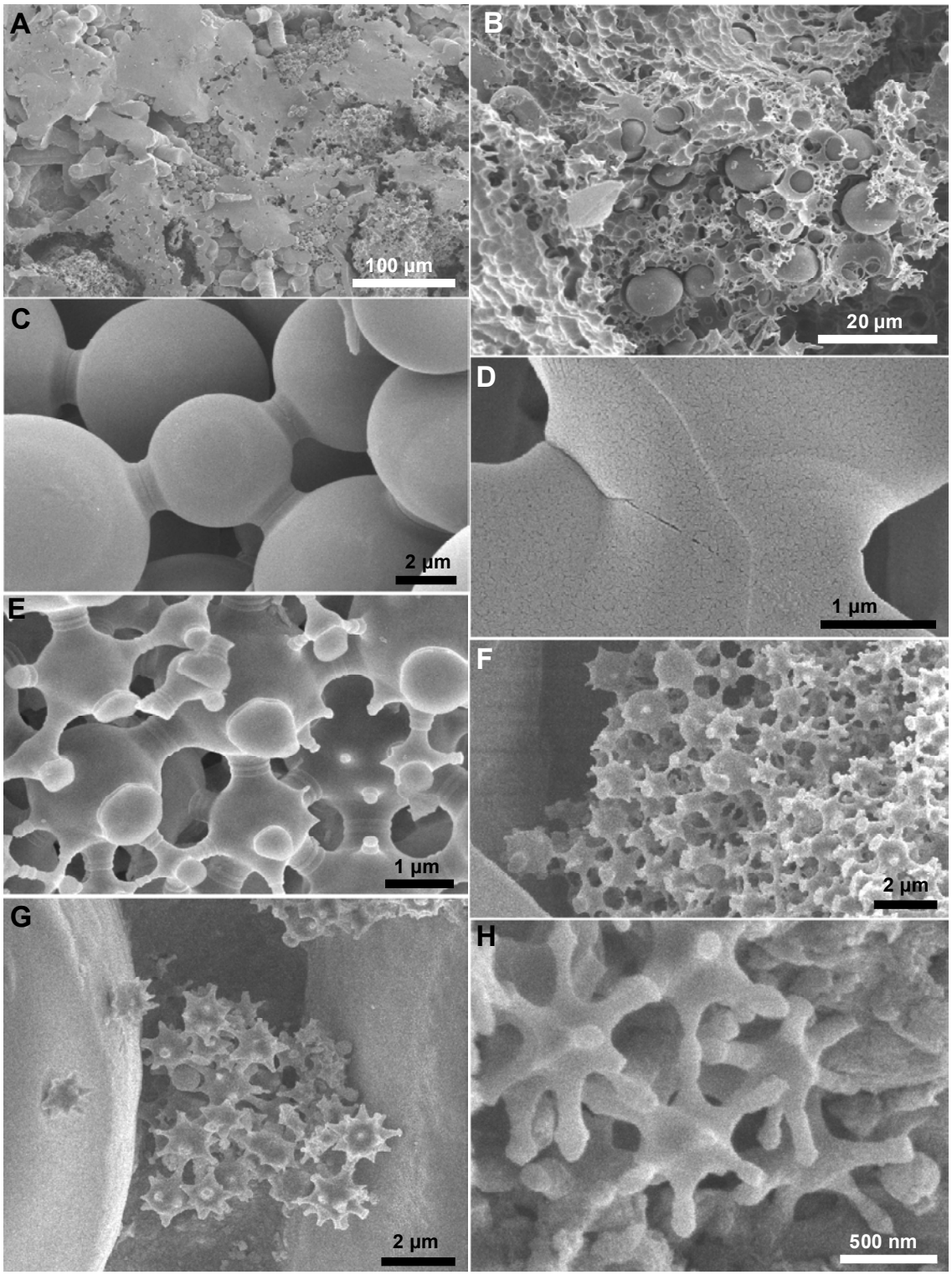

Figure 4: Dissolution of sinter via acidic steam condensate overprinting or ascending acid spring flow to form 'silica stars' in opal-A portions of the sinter. A) Differential dissolution of solid sinter mass to reveal silica-encrusted filaments; spheres once attached to filaments accumulated freely in pockets. B) Detail of concave dissolution pits in sinter mass and emergence of free silica spheres. C) Where silica spheres touched, necks formed to connect adjacent spheres. D) Detail of merged neck between two spheres. E) Double ring structures and 't-joints' formed between spheres with continuing dissolution. F-H) Further dissolution

formed star-shaped structures with elongated necks that thinned to points; in some cases stars broke free and accumulated in piles between less-affected spheres.

4. DISCUSSION AND SUMMARY

It has become evident that the mineralogical transformation from opal to quartz in siliceous sinter deposits proceeds at different rates in time and space. Moreover, quartz may form quickly, especially if environmental conditions change from alkaline to acid. Such circumstances are relatively common in geothermal fields in New Zealand, where lowering of the piezometric level over time at some locations has allowed infiltration of steam acid condensate into country rock, including old sinter deposits (e.g., Martin et al., 2000; Campbell et al., 2004). The consequences for preservation of microbial textures are not good, as has been shown in this study, as well as in field experiments by Lynne et al. (2006a) at nearby Orakei Korako.

The paragenesis of the siliceous matrix for any given sinter deposit reveals information about original paleoenvironmental conditions, including paleobiological content, broad temperature gradients of paleo-outflows, as well as changing thermal fluid history (cf. Walter, 1976: Cady and Farmer, 1996; Jones et al., 1997; Campbell et al., 2001; Guidry and Chafetz, 2003; Lynne and Campbell, 2003). At Sinter Island, early diagenetic sinter still preserves microbial textures, with filament diameters suggestive of moderate discharge temperatures. Three phases of alkali-chloride thermal fluid expulsion produced distinctive siliceous deposits that entombed the filaments. Transformation of the sinter has progressed, in places, through opal-CT, opal-C and quartz, with morphological and mineralogical changes occurring gradually and gradationally. At the physical margins of dense, white, quartzose (by XRPD analysis) horizons, incipient 'fuzzy' quartz microcrystals have grown into cavities. This 'baby quartz' clearly emerges from the moderately dense sinter mass as structural water is expelled and typical opal-C, rod-like nanostructures (cf. Lynne et al., 2005) realign and sharpen into criss-cross patterns aligned with future c-axes of the quartz microcrystals. Lynne et al. (in review) showed that crystallographic and morphologic signatures of quartz are imprinted on all precursor silica phases except noncrystalline opal. The arrangement of aligned morphologic features such as the criss-cross structures at Sinter Island is not random but represent orientations of future crystal faces (cf. Lynne et al., in review). This is the first study to capture detailed morphological transitions of the 'birth' of quartz in sinter deposits undergoing diagenesis.

Post-depositional dissolution modifies original (paleo)environmental signatures, and in extreme acid-overprinting, influences whether any siliceous product is preserved at all. At Sinter Island, opaline deposits have undergone a distinctive series of dissolution steps that reversed the three-part siliceous layering produced in the earlier alkali chloride thermal regime. 'Silica star' formation proceeds at the expense of smaller particles, with originally large spheres shrinking inward and spine-like bosses protruding wherever adjacent spheres once touched. When two silica particles collide they become bonded through the formation of inter-particle bonds that create siloxane bridges at the contact points. This process results in the formation of inter-particle necks. The necks provide sites of negative radius of curvature and the solubility at this point is low (Iler, 1979). In conditions such as those at Sinter Island, the acidic steam condensate lowered the pH, enhancing dissolution of silica which decreased particle sizes (Iler, 1979). The rate of phase transformations of a particle is faster for smaller particles because of the greater number of nucleation sites per unit volume. This process increases the energy available to overcome the restricting activation barriers. Hence, silica phase transformation rates are accelerated in these circumstances (Banfield and Hamers, 1997).

5. REFERENCES

Banfield, J.F., Hamers, R.J. (1979). Processes of minerals and surfaces with relevance to microorganisms and prebiotic synthesis. In: Banfield. J., Nealson, K. (Eds.), *Reviews in Mineralogy* 35. Geomicrobiology: Interactions between microbes and minerals, 81-122.

Bignall, G. (1991). Subsurface stratigraphy and structure of the Orakeikorako and Te Kopia geothermal systems: *Proceedings of 13th NZ Geothermal Workshop*, 199-205.

Cady, S.L., Farmer, J.D. (1996). Fossilization processes in siliceous thermal springs: trends in preservation along thermal gradients. In: Bock, G.R., Goode, J.A. (Eds.), Evolution of Hydrothermal Ecosystems on Earth (and Mars?): *Proceedings of the CIBA Foundation Symposium 202.* Wiley, Chichester, U.K., pp. 150-173.

Campbell, K.A., Buddle, T.F., and Browne, P.R.L. (2004). Late Pleistocene silica sinter associated with fluvial, lacustrine, volcaniclastic and landslide deposits at Tahunaatara, Taupo Volcanic Zone, New Zealand: *Transactions of the Royal Society of Edinburgh (Earth Sciences)*, Vol. 94, 485-501.

Campbell, K.A., Sannazzaro, K., Rodgers, K.A., Herdianita, N.R., and Browne, P.R.L. (2001). Sedimentary facies and mineralogy of the Late Pleistocene Umukuri silica sinter, Taupo Volcanic Zone, New Zealand: *Journal of Sedimentary Research*, Vol. 71, 728-747.

Currie, A.E. (2005). Prokaryotic communities of geyserite deposits surrounding a high temperature alkali chloride hot spring: Unpublished MSc Thesis, University of Auckland, Auckland, New Zealand, 133 p.

Guidry, S.A., Chafetz, H.S. (2003). Depositional facies and diagenetic alteration in a relict siliceous hot spring accumulation: examples from Yellowstone National Park, U.S.A: *Journal of Sedimentary Research* Vol. 73, 806-823.

Hamlin, K.A. (1999). Geological studies of the Orakeikorako geothermal field, Taupo Volcanic Zone: Unpublished MSc Thesis, University of Auckland, Auckland, New Zealand, 118 p.

Herdianita, N.R., Browne, P.R.L., Rodgers, K.A. and Campbell, K.A. (2000). Mineralogical and textural changes accompanying ageing of silica sinter: *Mineralium Deposita,* Vol. 35, 48-62.

Iler, R.K. (1979). The chemistry of silica: solubility, polymerization, colloid and surface properties, and biochemistry. John Wiley and Sons, New York, 866 p.

Jones, B., Renaut, R.W., Rosen, M.R. (1997). Vertical zonation of biota in microstromatolites associated with hot springs, North Island, New Zealand: *Palaios*, Vol. 12, 220-236.

Lloyd, E.F. (1972). Geology and hot springs of Orakeikorako: *New Zealand Geological Survey Bulletin* 85, 164 p.

Lynne, B.Y., Campbell, K.A. (2003). Diagenetic transformations (opal-A to quartz) of low- and mid-temperature microbial textures in siliceous hot-spring deposits, Taupo Volcanic Zone, New Zealand: *Canadian Journal of Earth Sciences,* Vol. 40, 1679-1696.

Lynne, B.Y., Moore, J., Browne, P.R.L., and Campbell, K.A. (2003). Age and mineralogy of the Steamboat Springs silica sinter deposit, Nevada, U.S.A.: a preliminary report of core SNLG 87-29: *Proceedings of 25th NZ Geothermal Workshop*, 65-70.

Lynne, B.Y., Campbell, K.A., Moore, J.N., and Browne, P.R.L. (2005). Diagenesis of 1900-year-old siliceous sinter (opal-A to quartz) at Opal Mound, Roosevelt Hot Springs, Utah, U.S.A.: *Sedimentary Geology*, Vol. 119, 249-278.

Lynne, B.Y., Campbell, K.A., Perry, R.S., Browne, P.R.L., and Moore, J.N. (2006a). Acceleration of sinter diagenesis in an active fumarole, Taupo Volcanic Zone, New Zealand: *Geology*, Vol. 34, 749-752.

Lynne, B.Y., Campbell, K.A., Browne, P.R.L., James, B., and Moore, J.N. (2006b). Siliceous sinter diagenesis: order among the randomness: *Proceedings of 28th NZ Geothermal Workshop*: this volume.

Lynne, B.Y., Campbell, K.A., James, B., Moore, J.N., and Browne, P.R.L. Tracking crystallinity in siliceous hot-spring deposits: *American Journal of Science*, in review.

Martin, R., Mildenhall, D., Browne, P.R.L., and Rodgers, K.A. (2000). The age and significance of in-situ sinter from the Te Kopia thermal area, Taupo Volcanic Zone, New Zealand: *Geothermics*, Vol. 29, p. 367-375.

Moar, N.T. (1993). Pollen Grains of New Zealand Dicotyledonous Plants: Manaaki Whenua Press, 200 p.

Simmons, S.F. and Browne, P.R.L. (1991). Active Geothermal Systems of the North Island, New Zealand; Guide Book for North Island Field Tour, IGCP Project 294: *Geological Society of New Zealand Miscellaneous Publication* 57, 70 p.

Walter, M.R, (1976). Hot-springs sediments in Yellowstone National Park. In: Walter, M.R. (Eds.), Stromatolites: Amsterdam, Elsevier, *Developments in Sedimentology,* 489-498.

6. ACKNOWLEDGEMENTS

This research was funded by the Royal Society of New Zealand, Marsden Fund. We thank Mr. and Mrs. Gibson for providing transport and allowing access to Sinter Island. Analytical equipment was supplied by the University of Auckland's Geology Department and Research Centre for Surface and Materials Science. Field and lab assistance was furnished by Andrea Alfaro, Aimee Currie, Kirsty Hamlin, Catherines Harris and Hobbis, Bryony James and Sue Turner.